INTENSITY AND GALACTIC ABSORPTION OF SOFT BACKGROUND X-RAYS

A. N. BUNNER, P. L. COLEMAN, W. L. KRAUSHAAR, D. McCAMMON,
T. M. PALMIERI, A. SHILEPSKY, and M. ULMER
Dept. of Physics, University of Wisconsin, Madison, Wis., U.S.A.

Abstract. Measurements of the soft X-ray background intensity show that the intensity is largest in that part of the sky where the columnar atomic hydrogen density is smallest. In the direction $b^{II} = -60°$, $l^{II} = 10°$ the intensity is found to be 195 ± 20 photons cm^{-2} sec^{-1} $ster^{-1}$ keV^{-1} near 0.26 keV and 20 ± 3 photons cm^{-1} sec^{-1} $ster^{-1}$ keV^{-1} near 0.9 keV. The intensity in the galactic plane is unexpectedly large.

We wish to report here recent new results on the intensity, angular distribution and possible origin of the soft X-ray background radiation. Our data are in partial agreement with the already-reported results of the Berkeley group (Bowyer *et al.* [1]) and the NRL group (Henry, *et al.* [2]), but are in rather serious disagreement with the results of the Calgary group (Baxter and Wilson [3]).

Two separate counter systems were flown, each of 250 cm^2 effective area and each with $2.6° \times 23°$ (FWHM) collimation. The principle axes of the two collimators were 180° apart and the counters were mounted so as to view perpendicular to the long axis of the slowly spinning and unguided Aerobee 150 rocket. The X-ray counters were separated from their veto counters by arrays of 0.005″ ground wires. This arrangement is very effective in reducing charged particle and γ-ray induced background. The window material of one counter was 4 micron 'Mylar', for the other 2 micron 'Kimfol'. Kimfol is a trade name for polycarbonate. The windows were coated on the inside with a very thin layer of colloidal carbon. Laboratory tests showed that the window material itself amply eliminated possible ultraviolet sensitivity. But at somewhat longer wavelengths where the windows became transmitting, we found that photoelectrons could be ejected from thin aluminum coatings. Carbon, with its high photoelectronic work function eliminated this potential source of malfunction. That ultraviolet and light sensitivity did not confuse our measurement was verified in flight through comparison of our data with the data from photometers prepared by the University's Space Astronomy Laboratory and flown on the same rocket.

The efficiencies of the two counters, plotted as functions of incident X-ray energy are shown in Figure 1. Notice that at 284 eV, the carbon K-edge, the Kimfol transmission is nearly three times that of the Mylar. In addition, the Kimfol transmission is large enough in the 500 eV to 1 keV region to permit measurements there, too. The data telemetered from each counter were accumulated counts for pulse heights corresponding to X-ray energies of 0.15 to 0.48, 0.48 to 0.96, 0.96 to 1.6, 1.6 to 2.65, 2.65 to 6.5 and 6.5 to 8.4 keV. An on-board retractable Fe^{55} calibration source demonstrated that the entire system including electronic gas regulator, high voltage, amplifier gains and level discriminators were stable to within 5% in measured X-ray

L. Gratton (ed.), Non-Solar X- and Gamma-Ray Astronomy, 342–351.

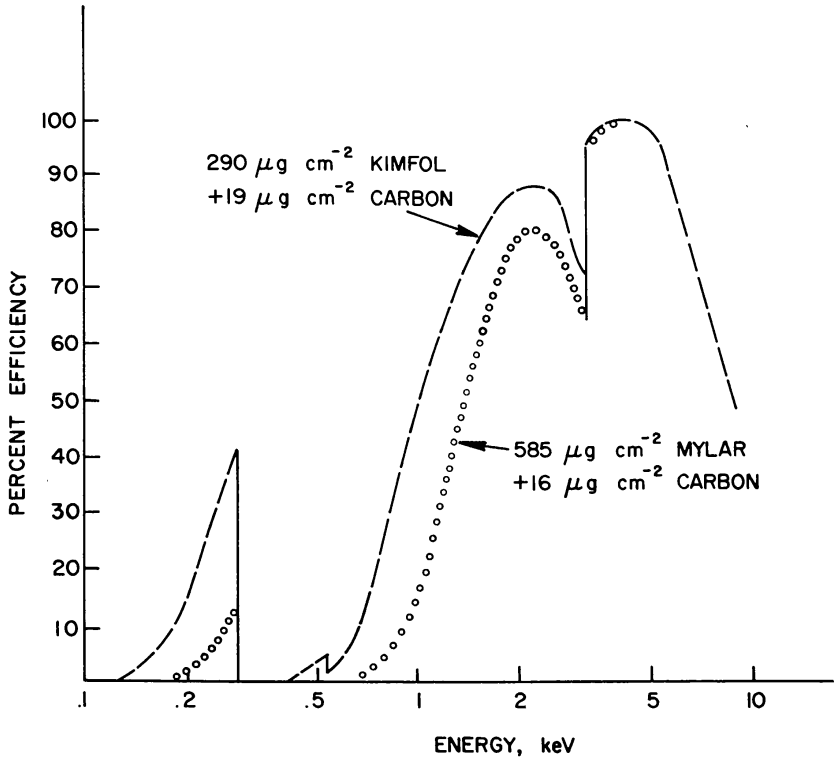

Fig. 1. Efficiency of the two counters vs. X-ray energy. Kimfol is $C_{16}H_{14}O_3$ and Mylar is $C_{10}H_8O_4$.

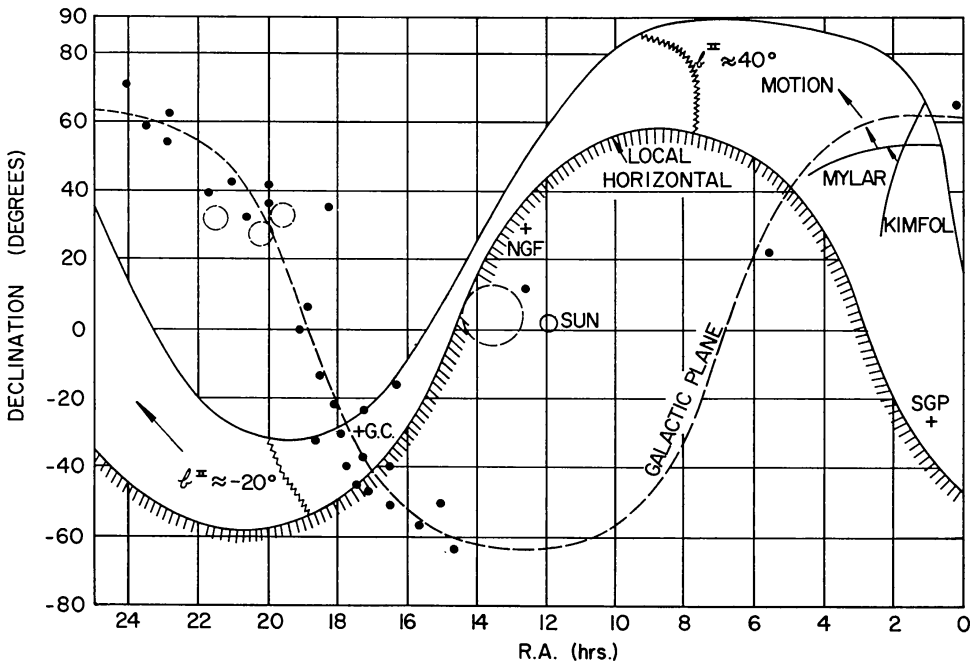

Fig. 2. Scan path in celestial coordinates. The black dots are approximate positions of known X-ray sources. The broken circles indicate regions of suspected enhanced soft X-ray emission. The large region near 14^{hr} is discussed by Bowyer *et al.* [1]; the three small regions near 20^{hr} are discussed by Henry *et al.* [2].

energy throughout the flight. The counters were flushed and refilled just prior to launch, and for several hours prior to launch counting gas was continuously forced through the payload section under a slight positive pressure.

The portion of the sky scanned is shown in Figure 2. Some discrete sources were crossed and their energy spectra are being studied. Only the region between $b^{II} \approx -20°$, $l^{II} \approx 340°$ and $b^{II} \approx 40°$, $l^{II} \approx 160°$ was used for the diffuse X-ray analysis to be discussed here.

We have used only the data taken near the south galactic pole to study the diffuse X-ray intensity in the region 1–8 keV. We find that in this region our data fit best an $E^{-1.5}$ power law and the absolute intensity as found by us is in good agreement with that found by others. See, for example, the summary plot of Gorenstein *et al.* [4]. As will be discussed further below, our data in the two lowest energy pulse height channels indicate the need for some sort of soft X-ray source in addition to the extrapolated power law. To emphasize this point, we have forced a fit of an $E^{-1.7}$ power law to the data for $E > 1$ keV and show the result together with all the high galactic latitude data points in Figure 3. The plotted points represent X-ray flux incident on the detector. *No corrections for interstellar absorption have been made.* Also shown in Figure 3 is the power law which *best* fits our data above 1 keV, $E^{-1.5}$. In any case, particularly because the data themselves show clearly the presence of interstellar absorption, it seems clear that our soft X-ray data cannot be explained by a power law extrapolation alone.

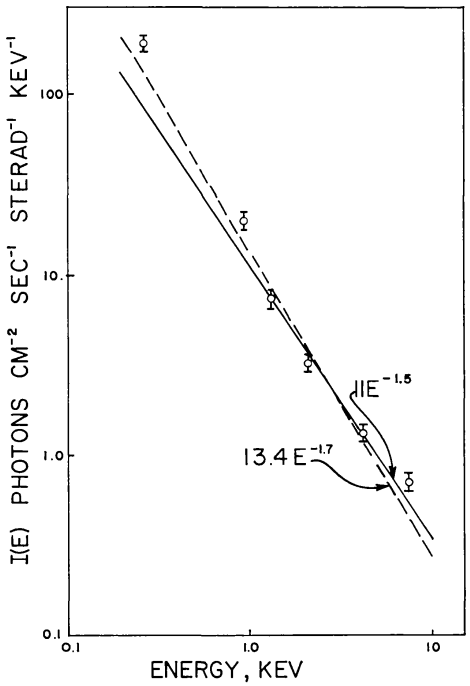

Fig. 3. X-ray intensity incident on the detectors vs. X-ray energy. The data used here were taken at high galactic latitudes, and no absorption effects have been included. The $E^{-1.5}$ power law fits our data best for $E > 1$ keV. The $E^{-1.7}$ power law is shown for comparison.

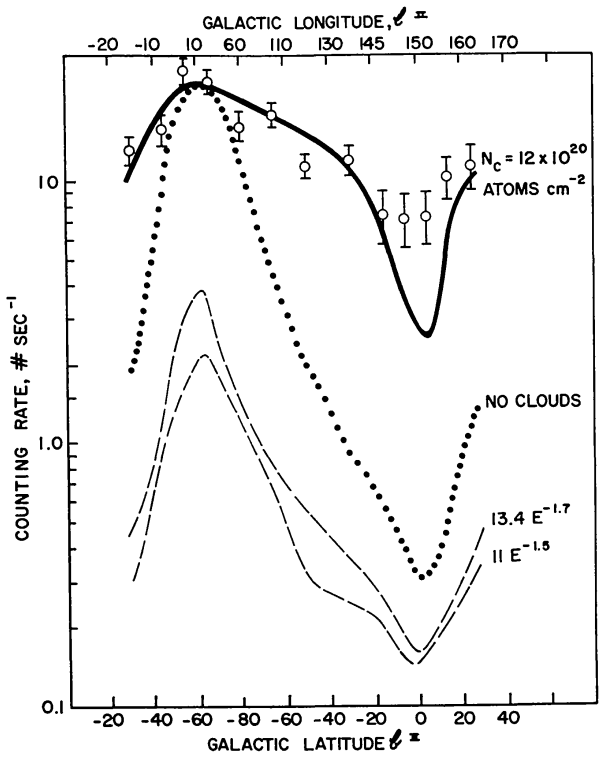

Fig. 4. Kimfol counter data in the 0.15 to 0.48 keV channel plotted vs. scan path in galactic coordinates. A background of 2.9 ± 0.3 sec^{-1} has been subtracted. Predicted curves are described in the text.

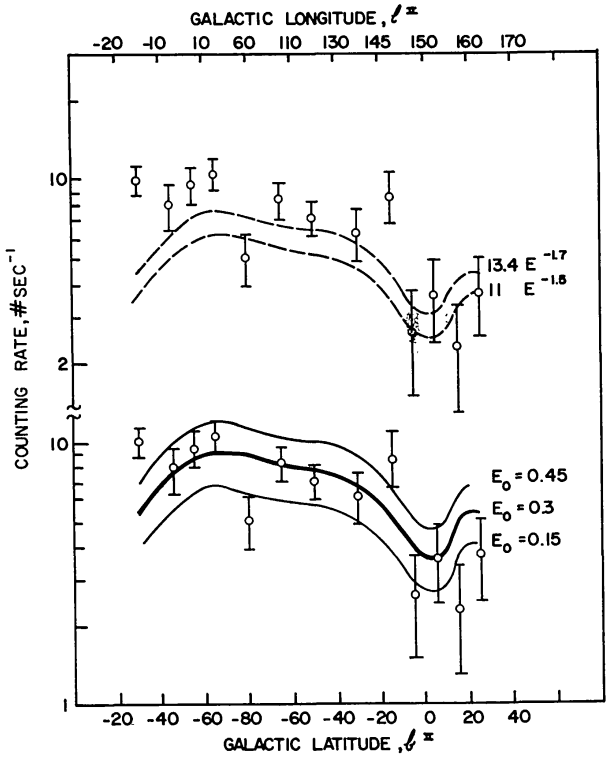

Fig. 5. Kimfol counter data in the 0.48 to 0.96 keV channel plotted vs. scan path in galactic coordinates. A background of 1.8 ± 0.2 sec^{-1} has been subtracted.

Figures 4 and 5 show the counting rates (Kimfol window counters) in the 0.15 to 0.48 and 0.48 to 0.96 keV pulse height channels respectively, plotted vs. position along the scan path. Galactic latitude is shown on the bottom scale, galactic longitude on the top. Data from the Mylar window counter are entirely similar, but the rates and statistical accuracy are less. Background rates of 2.9 ± 0.3 sec^{-1} and 1.8 ± 0.2 sec^{-1} have been subtracted from the two low energy channels. These background rates ware taken when the collimators viewed the earth. Table I shows a summary of the

TABLE I

Measured background rates

Altitude	Direction	Detector window	Measured rates sec^{-1}	
			0.15–0.48 keV	0.48–0.96 keV
80 km[a]	(Doors on)	Kimfol	3.8 ± 0.6	2.3 ± 0.4
80 km[a]	(Doors on)	Mylar	3.0 ± 0.5	2.4 ± 1.4
80 km[a]	up	Kimfol	2.9 ± 0.7	1.6 ± 0.5
80 km[a]	up	Mylar	2.5 ± 0.5	2.3 ± 0.4
80 km[a]	down	Kimfol	2.9 ± 0.4	1.7 ± 0.3
80 km[a]	down	Mylar	1.5 ± 0.4	1.5 ± 0.4
80 km[b]	up	Kimfol	3.9 ± 0.6	1.4 ± 0.5
80 km[b]	up	Mylar	4.1 ± 0.6	2.1 ± 0.5
80 km[b]	down	Kimfol	2.3 ± 0.4	1.9 ± 0.4
80 km[b]	down	Mylar	1.9 ± 0.4	1.3 ± 0.3
>140 km	down	Kimfol	2.9 ± 0.3	1.8 ± 0.2
>140 km	down	Mylar	2.8 ± 0.3	1.6 ± 0.2

[a] Rocket ascending.
[b] Rocket descending.

background rates, evaluated in different ways. The scatter is perhaps a little greater than what one would expect if all were independent measures of the same quantity, but we regard the consistency and small relative magnitude of the background as good evidence that our soft X-ray measurements are not seriously contaminated with, for example, an anamolous charged particle background.

The measured ratio of the Kimfol transparency to that of the Mylar is 2.7 ± 0.3 at the carbon edge. At lower energies the Kimfol is more transparent than the Mylar by an even larger factor and for most of the spectra we have considered the predicted counting rates in the first channels of the Kimfol and Mylar counters are in the ratio 5 to 1. The measured rates, however, after background subtraction, are in the ratio 2.7 ± 0.2. We understand the origin of a large fraction of this apparent discrepancy. The window materials were mounted behind polished aluminum frames into which had been milled 3/16″ wide slots. Particularly the Mylar stretched and bulged up

under pressure into these slots and so produced, in effect, a non-uniform window thickness. The centers of the bulges were more transparent than the original flat material on which the transparencies were measured. We have evaluated the effect in the laboratory and when all uncertainties are included the predicted ratio becomes 3.6 ± 0.6 (rather than 5) to be compared with the measured value in flight of 2.7 ± 0.2. This state of affairs is admittedly not entirely satisfactory and will be investigated further.

The data plotted in Figure 5 and particularly in Figure 4 show clearly the effects of interstellar absorption. The highest counting rate encountered along the scan path occurs at the position of least atomic hydrogen, as measured in the 21 cm emission surveys [5]. In both figures the broken lines represent predicted counting rates given (i) the extrapolated power law spectra incident from outside the Galaxy, (ii) galactic absorption calculated from the effective cross sections compiled by Bell and Kingston [6] and (iii) columnar hydrogen density as summarized by Kerr and Westerhout [5]. (An outline of the procedures used in making these and other predictions is shown in Table II.) The dotted curve in Figure 4 shows the effect of simply in-

TABLE II

Analysis procedure

1. X-ray spectrum incident on galaxy
   $A E^{-\gamma} + B/E \exp(-E/E_0)$.
2. Attenuation by interstellar gas
   (a) Kerr and Westerhout [5] N_H contours;
   (b) Bell and Kingston [6] σ;
   (c) Evaluate $e^{-\tau}$ at 9 points along collimator.
3. Evaluate atmospheric attenuation (exclude if $> 10\%$ effect).
4. Results of (1, 2 and 3 above) is predicted X-ray spectrum incident on counter windows.
5. Multiply 4 above by counter window and gas efficiency.
6. Evaluate transfer effects in counter (Argon escape peak).
7. Result is predicted pulse height spectrum in counter with perfect resolution.
8. Fold 7 above with counter resolution.
9. Integrate 8 above over pulse height bins.

I	II	III	IV	V	VI
0.15–0.48	0.48–0.96	0.96–1.6	1.6–2.65	2.65–6.5	6.5–8.4

10. Result is predicted counting rate in each pulse height bin at one time in flight.
11. Procedure repeated at 0.5 sec intervals ($\simeq 9°$) through useful portion of flight.
12. Average predictions over repeated scans of same part of sky to compare with observations.

creasing the assumed incident soft X-ray intensity so as to fit the observations at the high counting rate point.* The dependence of the observations on galactic latitude is much weaker than predicted. That is, there is too little apparent absorption, as already pointed out by Bowyer *et al.* [1].

* Note that this dotted curve is not just the lower curve scaled by a constant factor. A portion of the counting rate in the 0.15 to 0.48 keV channel, particularly near the galactic plane, has its origin in the argon K_α escape phenomena excited by X-rays near 3 keV. This effect with the Kimfol window counter is relatively small. With the Mylar window counter it is large and tends to obscure deep absorption features.

1. Anomalous Apparent Absorption

We have considered in our analysis a number of possible explanations for the unexpected weak dependence of the soft X-ray intensity on galactic latitude.

(a) If there were less actual gas than indicated by the 21 cm surveys or if the helium content of the interstellar medium were less than was assumed by Bell and Kingston [6], there should be too little apparent absorption in the 0.48 to 0.96 keV measurements also. To within the rather poor statistical accuracy of our measurements in this region (see Figure 5) this seems not to be the case.

(b) If the interstellar gas were concentrated in small dense clouds rather than distributed more or less smoothly as was assumed in making the previous predictions, the X-ray absorption would be less. Bowyer and Field [7] have also considered this possibility. The apparent absorption of X-rays by gas of columnar density N_H distributed not uniformly but in randomly-positioned clouds of columnar density N_c each is described by an optical depth

$$\tau_e = (N_H/N_c)\,[1 - \exp(-N_c\sigma)], \tag{1}$$

where σ is the energy-dependent absorption cross section. We find that hypothetical clouds of $N_c \approx 12 \times 10^{20}$ atoms cm^{-2} are required to produce absorption in reasonable agreement with that observed. The bold solid curve of Figure 4 has been computed under this assumption. (The incident spectrum assumed for this case was $11\,E^{-1.5} + (100/E)\exp(-E/0.3)$, and will be discussed later.) This value of N_c is very large and while there is perhaps some support for dense clouds structures [8, 9, 10], we feel it appropriate to examine less severe assumptions.

(c) If there were some unsuspected source of isotropic soft X-rays of terrestial or solar origin, an otherwise highly anisotropic flux would appear less so. In this case we should subtract the observed flux level near $b^{II}=0$ from all observations, and the data treated in this way are shown in Figure 6. As in Figure 4, the two dashed lines show predicted rates for extrapolated power law spectra, normal interstellar absorption having been assumed. The dotted curve, again as in Figure 4, shows the effect of increasing the assumed incident soft X-ray intensity so as to fit the observations at the high counting rate point. Even here, the observed and predicted dependence on galactic latitude are not in agreement. There is too little absorption. Now, however, clouds of only $N_c \approx 4 \times 10^{20}$ atoms cm^{-2} are required to match the absorption, and the bold solid curve has been calculated for clouds of this thickness. The incident spectrum is the same as that assumed before, $11\,E^{-1.5} + (100/E)\exp(-E/0.3)$. That the second term is the same as before is accidental.

(d) The very steep dependence of the predicted soft X-ray intensity on galactic latitude is a direct consequence of our assumption that the soft X-ray source is extragalactic. If the soft X-ray emission were of galactic origin the intensity variation with galactic latitude would depend on how the supposed emission was distributed relative to the gas. In order to examine this possibility we have assumed gaussian distributions in height, z, above the galactic plane for the gas and emission and have

for the predicted intensity

$$I = S_0 \int_0^{\infty} \exp - \left(\frac{r}{z_s \sin b} \right)^2 e^{-\tau} \, dr, \tag{2}$$

where

$$\tau = \sigma n_0 \int_0^{r} \exp - \left(\frac{r'}{z_g \sin b} \right)^2 dr' .$$

S_0 is the source strength, z_g and z_s characterize the gas and emission distributions in z, respectively, σ is the soft X-ray absorption cross section and n_0 is the gas density

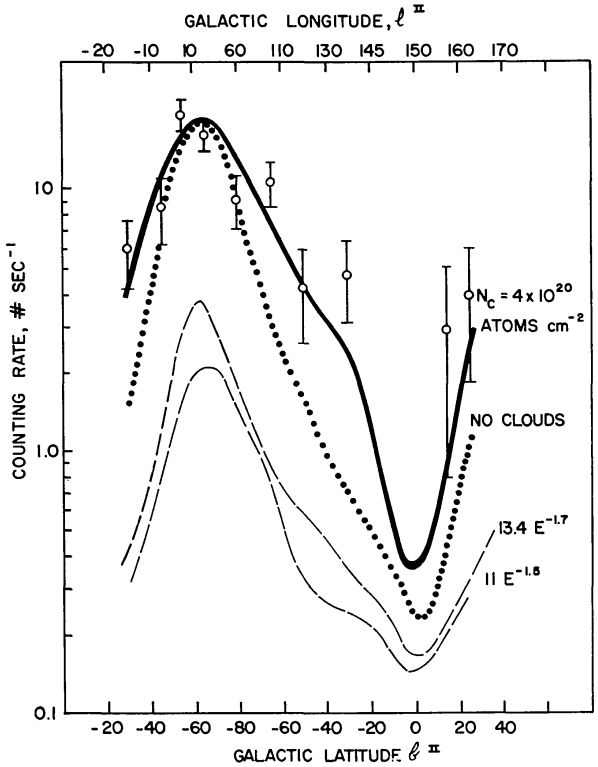

Fig. 6. Kimfol counter data in the 0.15 to 0.48 keV channel plotted as in Figure 4. Here in addition to the 2.9 ± 0.3 sec^{-1} background, the observed rate near $b^{II} = 0$ has been subtracted as background. Predicted curves are discussed in the text.

in the galactic plane. Approximate fits to the latitude dependence of the data in our lowest energy channel (0.15 to 0.48 keV) can be obtained with $n_0 = 1$ cm^{-3}, $z_s = 400$ pc, $z_g = 94$ pc and $S_0 = 4 \times 10^{-19}$ photons cm^{-3} sec^{-1} sterad^{-1} keV at 0.26 keV. The value of S_0 is very large and corresponds to about 13 objects of the soft X-ray luminosity of the sun (quiet sun at solar maximum) per cubic parsec. The value of z_g corresponds to about 160 pc between half-density points either side of the galactic plane and while appreciably smaller than Schmidt's [1] value of 220 pc, is comparable

with more recent estimates [5]. The value of z_s, 400 pc, is entirely reasonable for Population II objects.

2. Soft X-Ray Spectrum

With only two broad band energy windows we cannot, of course, determine a precise spectral shape. There is, however, evidence for an intensity above that attributable to an extrapolated power law in the 0.48–0.96 keV pulse height channel as well as the lowest energy channel and this provides some spectral information. We have chosen rather arbitrarily to fit our data to incident spectra of the form $AE^{-\gamma}+BE^{-1}$ exp $(-E/E_0)$ – a power law, the normalization and index of which are established by measurements at $E>1$ keV, and a free-free spectrum with constant Gaunt factor. Under a given set of assumptions, data from the first or low energy channel determine possible combinations of B and E_0 and data from the second channel determine E_0, or a temperature. Quite accidentally, the required values of B and E_0 are the same whether we treat the data as in (b) above (subtract just the background as found from earth scans) or as in (c) above (subtract the observed intensity near $b^{II}=0$ as a 'background'.) The sensitivity of the measurement to assumed values of E_0 is shown by the bottom set of curves of Figure 5. Because the input spectra are the same for

TABLE III

Values of B and E_0

Case (b), $N_c = 12 \times 10^{20}$ atoms cm^{-2}		
γ	B	E_0
1.5	100	0.30
1.7	68	0.30
Case (c), $N_c = 4 \times 10^{20}$ atoms cm^{-2}		
γ	B	E_0
1.5	100	0.30
1.7	70	0.30

cases (b) and (c), and because even clouds of $N_c=12\times10^{20}$ atoms cm^{-2} have very little effect on the absorption of X-rays that contribute to the observations in the second channel, the curves in the bottom part of Figure 5 are appropriate to both cases. We conclude that under these assumptions, E_0 is near 0.30 keV and values as small as 0.15 keV or as large as 0.45 keV are probably excluded.

We have repeated the entire procedure for a power law of index 1.7. The temperature or E_0 sensitivity is about the same as with a 1.5 power law index, and values of B and E_0 are shown in Table III.

3. Summary

The maximum soft X-ray intensity we observe is in the direction $b^{II}\approx-60°$, $l^{II}\approx10°$

and coincides with the direction in which the columnar atomic hydrogen density is smallest. Near 0.26 keV the measured intensity is

$$I = 195 \pm 20 \text{ photons cm}^{-2} \text{ sec}^{-1} \text{ ster}^{-1} \text{ keV}^{-1}$$

and near 0.9 keV is

$$I = 20 \pm 3 \text{ photons cm}^{-2} \text{ sec}^{-1} \text{ ster}^{-1} \text{ keV}^{-1}.$$

The corresponding values near the galactic plane ($b^{II} \approx 0$, $l^{II} \approx 155°$) are, near 0.26 keV

$$I = 57 \pm 8 \text{ photons cm}^{-2} \text{ sec}^{-1} \text{ ster}^{-1} \text{ keV}^{-1}$$

and near 0.9 keV

$$I = 6 \pm 1.5 \text{ photons cm}^{-2} \text{ sec}^{-1} \text{ ster}^{-1} \text{ keV}^{-1}.$$

The quoted uncertainties include counting statistics and estimated systematic errors such as uncertainties in window thickness, background subtraction, etc.

If we ignore for the moment the possibility that galactic objects contribute to the soft X-rays observed, our data imply an extragalactic component with an intensity given by

$$I = 11E^{-1.5} + 100E^{-1} \exp(-E/0.30) \text{ [photons cm}^{-2} \text{ sec}^{-1} \text{ ster}^{-1} \text{ keV}^{-1}]$$

(E in keV)

It should be emphasized that we have by no means established the analytic form of this expression. The first term is just the power law spectrum extrapolated to low energies, the second term a convenient computational device.

Acknowledgements

It is a pleasure to acknowledge the essential contributions of the Sounding Rocket Branch of the Goddard Space Flight Center and the financial support provided by NASA under grant NGR 50-002-044.

References

[1] Bowyer, C. S., Field, G. B., and Mack, J. E.: 1968, *Nature* **217**, 32.
[2] Henry, R. C., Fritz, G., Meekins, J. F., Friedman, H., and Byram, E. T.: 1968, *Astrophys. J. Lett.* **153**, L199.
[3] Baxter, A. J., Wilson, B. G., and Green, D. W.: 1969, *Astrophys. J. Lett.* **155**, L145.
[4] Gorenstein, P., Kellogg, E. M., and Gursky, H.: 1969, *Astrophys. J.* **156**, 315.
[5] Kerr, F. J. and Westerhout, G.: in *Galactic Structure*, Vol V. of *Stars and Stellar Systems* (ed. by A. Blaauw and Schmidt), University of Chicago Press, Chicago and London.
[6] Bell, K. L. and Kingston, A. E.: 1967, *Monthly Notices Roy. Astron. Soc.* **136**, 241.
[7] Bowyer, C. S. and Field, G. B.: 1969, *Nature* **223**, 573.
[8] Heiles, C.: 1967, *Astron. J.* **72**, 1040.
[9] Makova, S. P.: 1965, *Soviet Astron-A.J.* **8**, 485.
[10] Grahl, B. H.: 1960, Mitt. Univ.-Stern. Bonn, No. 28.
[11] Schmidt, M.: 1957, *Bull. Astron. Inst. Neth.* **13**, 247.